ISSN 2580-0817

Simulation of Stress, Deformation, and Vibration in Unlubricated Ball Bearings at Varying Rotational Speeds

Billy Dwiki, Moh. Hartono*

Department of Mechanical Engineering, Malang State Polytechnic,
Jl. Soekarno HattaNo. 9, Malang, 65141, Indonesia
**Corresponding author:moh.hartono@polinema.ac.id*

Article history:
Received: 6 June 2025 / Received in revised form: 10 July 2025 / Accepted: 15 July 2025
Available online 7 September 2025

ABSTRACT

Bearings are critical components in rotating machinery, and their performance is highly influenced by operational factors such as rotational speed, load, and lubrication. This study aims to analyze the deformation, stress, and dynamic behavior of SAE 52100 bearings under dry operating conditions at various rotational speeds, as well as to propose mitigation strategies for high-speed industrial applications. A finite element simulation was conducted using ANSYS R19.2 to evaluate the total deformation, equivalent elastic strain, Von Mises stress, and vibrational characteristics of a 6204-type SAE 52100 bearing. The simulations were performed across a speed range of 600 to 2000 RPM under dry conditions. The model incorporates standard mechanical properties of SAE 52100 steel and replicates real operational geometry and load scenarios. The results indicate that both deformation and stress levels increase significantly with speed, with critical concentrations occurring at the inner raceway and ball contact regions. Resonance phenomena were observed around 1100 RPM, leading to high-amplitude vibrations and localized structural strain. Von Mises stress rose non-linearly with speed, suggesting elevated risks of fatigue failure. The absence of lubrication exacerbates wear, heat generation, and mechanical instability. This study highlights the importance of effective lubrication, vibration monitoring, and design optimization. Future work should incorporate thermal effects, transient loads, and experimental validation to enhance the applicability of the findings for predictive maintenance strategies in high-speed machinery.

Keywords: *Dry contact, equivalent elastic strain, finite element analysis, resonance, SAE 52100 bearing, tribology, vibration.*

I. Introduction

Bearings are critical components in rotating machinery, responsible for supporting radial and axial loads while ensuring stable rotation. Their performance is highly sensitive to operational factors such as high rotational speeds, dynamic loading, and inadequate lubrication—all of which contribute to surface degradation and structural failure [1]. SAE 52100 steel is widely used in bearing applications due to its high hardness, excellent fatigue resistance, and dimensional stability, making it well-suited for high-speed and long-duration industrial operations.

Bearing defects usually need to be detected long before they cause any catastrophic system failure. If unplanned downtime is what one would prefer to avoid, then this would also mean an early detection of the faults. It is in this respect that numerical simulation techniques have found growing application as an efficient tool for performance assessment of bearings under different loading and lubrication conditions [2]-[5]. Simulations like these allow for very broad-based consideration of matters such as dynamic response, stress-strain

DOI: 10.17977/um016v9i22025p368

distribution, and surface contact behavior matters which are typically extremely difficult to observe through normal experimental means [6].

Several dynamic models have been developed to analyze the vibration characteristics of spindle systems containing defective bearings [7]. These models account for different defect types such as dents, spalls, and surface irregularities, which result in complex vibration patterns when multiple defects are present. Analytical models, particularly those applied to spherical roller bearings with localized faults, have demonstrated accurate prediction of vibrational behavior based on defect size and location [8]. Moreover, Modelica-based simulation environments have been employed to generate synthetic fault data for training machine learning algorithms, especially in cases where experimental datasets are limited [9].

Previous studies have shown that vibration analysis is a reliable diagnostic technique for identifying bearing defects. Characteristic defect frequencies, inner race defect frequency, and fundamental fault frequencies are major indicators for condition monitoring [10]. Rotational speed, defect size, and radial load have been found to affect the amplitude distributions and the frequency components. Statistical methods based on vibration energy and kurtosis values have also been used to assess defect severity in various operating conditions [11]. Another study reported that the combined approach of edited cepstrum, resampling, local mean decomposition (LMD), and continuous wavelet transform (CWT) was effective for filtering and measuring the width of OR defects at varying speeds [12]. Finite element analysis also indicates that rotational speed, load, and defect dimensions are influential in the maximum stress concentration in bearing structures.

In light of these studies, the present study aims to analyze the effects of dry operating conditions on SAE 52100 bearings at various rotational speeds, focusing on deformation, stress distribution, and dynamic response. The findings of this study are highly relevant to a broad range of high-technology applications, including aerospace propulsion systems, offshore wind turbines, and precision medical equipment, where mechanical reliability under extreme conditions is a critical determinant of system performance. Furthermore, the research opens avenues for the development of next-generation bearing materials with superior wear resistance and thermal stability, while laying the scientific foundation for condition-based predictive maintenance systems supported by real-time monitoring technologies.

II. Material and Methods

Material

SAE 52100 bearings consist of bearing components made of SAE 52100 steel, including inner rings, outer rings, and bearing balls. This bearing has a Young's Modulus Value of 208,000 MPa, reflecting the high stiffness of the material, while the density of 7,850 kg/m³ shows the typical properties of alloy steel. Poisson's Ratio of 0.30 and a coefficient of thermal expansion of 10×10^{-6}/K are standard values for steel materials. The flexural strength reaches 2,400 MPa, indicating excellent resistance to bending loads. Thermal conductivity ranges from 30-40 W/mK, indicating a fairly good heat conduction ability. The stress cycle parameter of 10×10^{7} cycles (50% failure) indicates high fatigue resistance, important for applications with cyclic loads [13].

Simulation Procedure

This research uses a simulation method with several parameters, as shown in Table 1. As in Table 1, the study used a simulation method to predict the probability of defects occurring in bearings. The SAE 52100 bearing type with a speed range of 600 - 2000 RPM was chosen because it is a widely used bearing steel and is known to have high hardness, fatigue resistance, and dimensional stability [14],[15]. This study began by designing bearing type SAE 52100 according to the standards in Autodesk Inventor 2016 software, then converted to be simulated to determine the bearing characteristics in Ansys software version R19.2. After the results were known, an analysis was carried out to further draw conclusions. The SAE 52100 type bearing used has the number 6204, which has dimensions of inner ring diameter of 20 mm, outer ring diameter of 47 mm, and bearing width of 14 mm. A radial load of 1,000 N was applied to the inner ring to simulate operational conditions, while the outer ring was fixed to emulate the stationary housing. Frictional contact (coefficient of friction = 0.15) was defined between the rolling elements and raceways to replicate dry operating conditions.

Table 1. Parameters of simulation

Parameters of simulation	
Mesh Size (mm)	2
Bearing Types	Sae 52100
Lubricants Condition	Dry
Material	Steel
Rotational Speed (RPM)	600; 800; 1300; 1500; 1700; 2000

A structured mesh with a 2 mm element size was generated, and mesh quality parameters (e.g., skewness < 0.25) were verified to ensure accuracy and convergence [16]. Simulations were conducted using the nonlinear static solver with large deflection and contact options enabled. The bearing system was simulated at rotational speeds ranging from 600 to 2000 RPM, and outputs including total deformation, equivalent elastic strain, and Von Mises stress were extracted for analysis.

III. Results and Discussions

Structural Response

As shown in Figure 1, the simulation results of the total deformation of the SAE 52100 type bearing without lubrication show a pattern of increasing deformation as the rotational speed increases from 600 to 2000 RPM. The deformation scale seen in the simulation results ranges from 0 mm (Min) to 5.566×10^{-6}/mm (Max), indicating the magnitude of nodal displacement due to centrifugal force and unlubricated contact that occurs in the system [17]. At 600 RPM (a), the maximum deformation of 5.566×10^{-6}/ mm appears locally in the contact area of the bearing ball with the inner raceway, with the affected area still predominantly dark blue (0 to 1.259×10^{-6}/ mm), indicating a low level of deformation. This indicates that at low speeds, even without lubrication, centrifugal force has not contributed significantly to producing deformation, and the contact is still stable with relatively small local stresses [18].

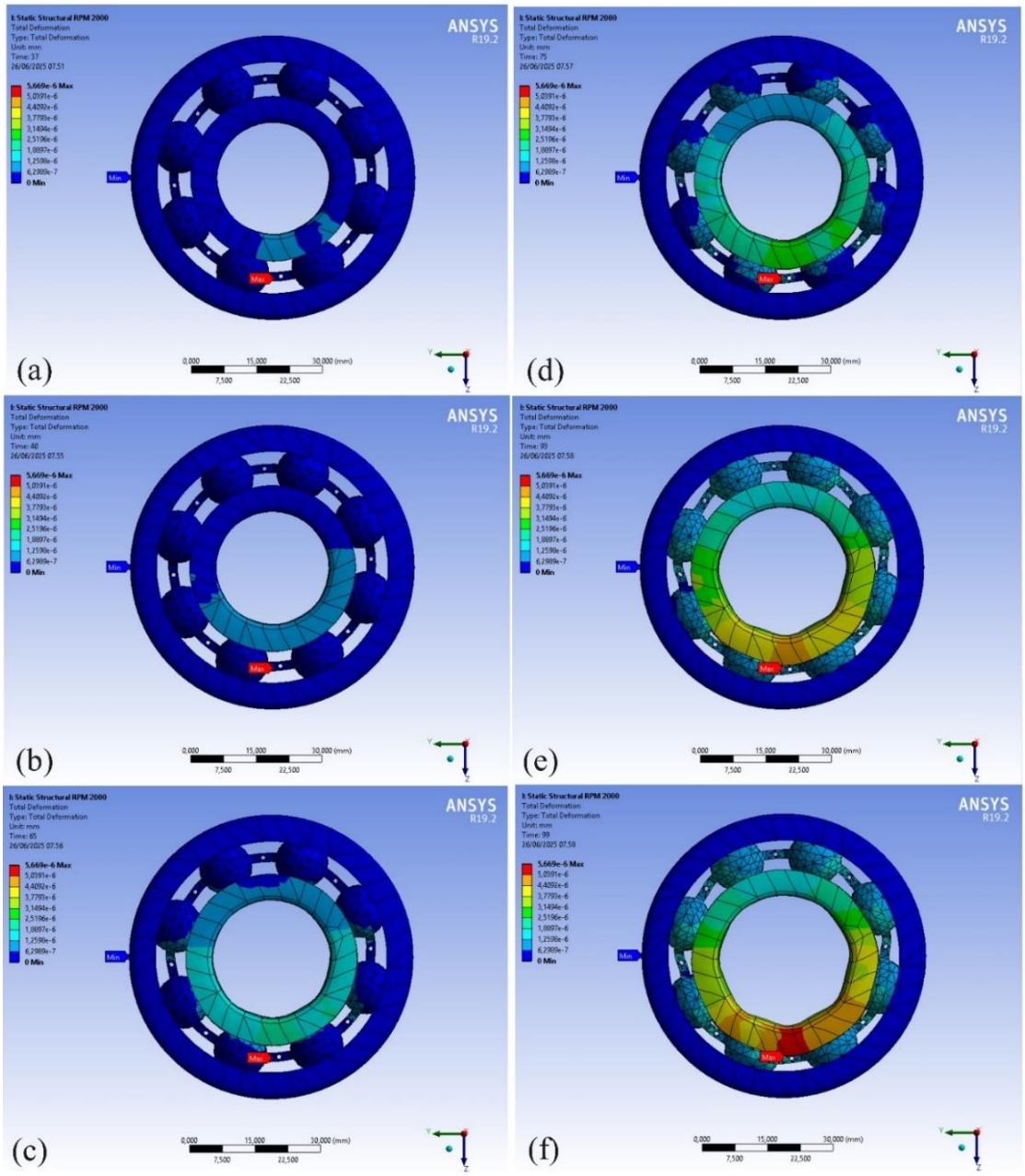

Fig. 1. Deformation simulation results at rotational speed : (a) 600 RPM, (b) 800 RPM, (c) 1300 RPM, (d) 1500 RPM, (e) 1700 RPM, and (f) 2000 RPM

As shown in Figure 2, the simulation results show that SAE 52100 bearings operating without lubrication experience a significant increase in the equivalent elastic strain distribution as the rotational speed increases from 600 RPM to 2000 RPM. The scale of the equivalent elastic strain values in this figure ranges from 5.3408×10^{-13}/ mm/mm (Min) to 6.4943×10^{-7}/ mm/mm (Max), which is consistent across all RPM conditions, but the color distribution and affected area show a different trend compared to the lubricated bearing condition.

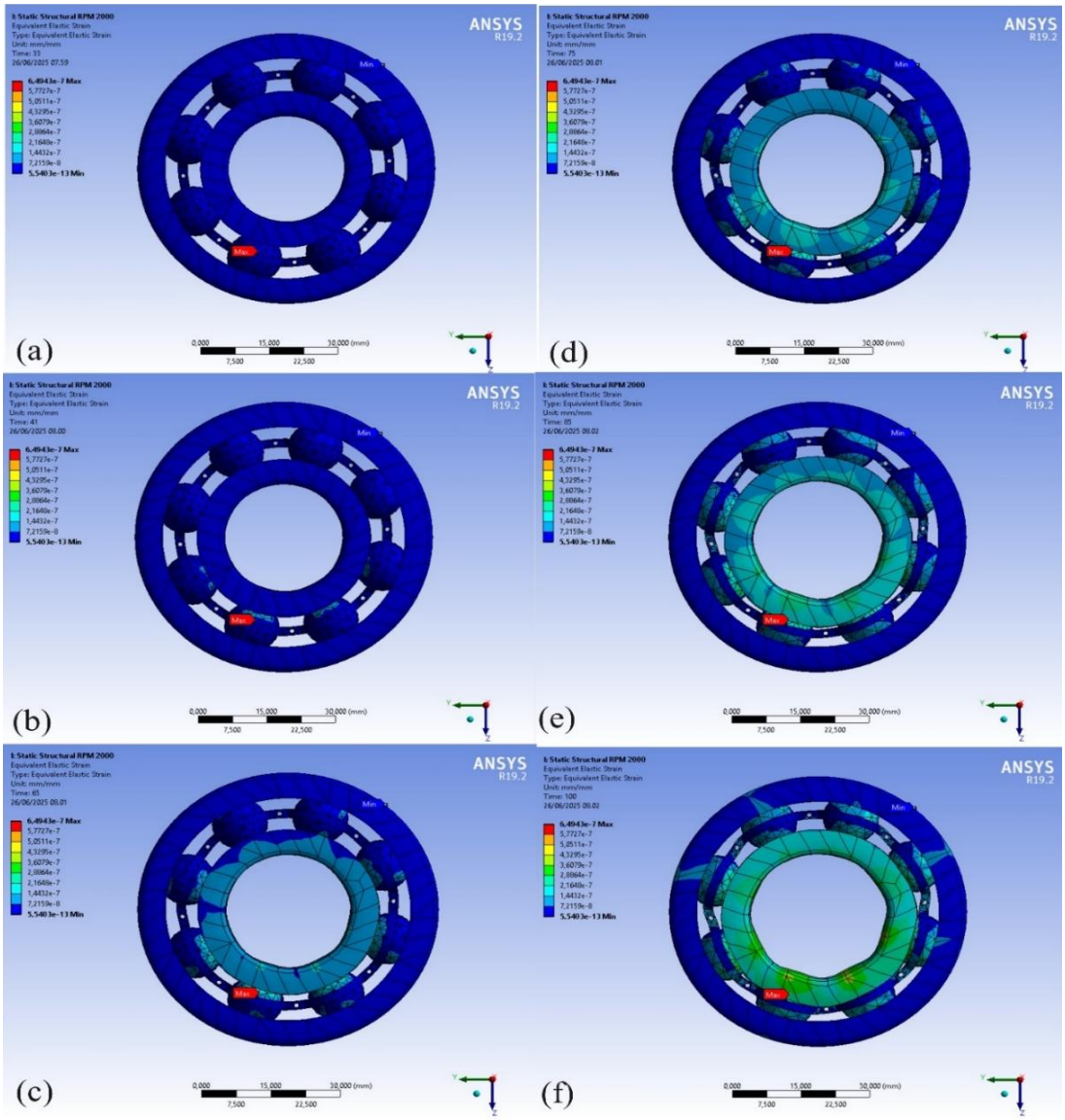

Fig. 2. Equivalent elastic simulation results at rotational speed : (a) 600 RPM, (b) 800 RPM, (c) 1300 RPM, (d) 1500 RPM, (e) 1700 RPM, and (f) 2000 RPM

As shown in Figure 3, as speed increases from 600 to 2000 RPM, the equivalent elastic strain in SAE 52100 bearings grows significantly, with strain distribution shifting from dark blue to reddish-yellow, indicating rising contact pressure and deformation. Metal-to-metal friction becomes dominant, causing increased heat, wear, and risk of fatigue failure [19]. This reduces bearing life, increases vibration, and lowers energy efficiency. Solutions include applying proper lubrication, regular maintenance, material and surface optimization, and rotational balancing [20].

Based on the simulation results of Von Mises stress against rotational speed (RPM) on SAE 52100 type bearings without lubrication. As shown in Figure 3, there is a significant increase in stress as the RPM increases. The graph shows a non-linear curve that tends to be exponential, where the Von Mises stress increases from around 1.00×10^{-2} MPa at 600 RPM to almost 1.15×10^{-1} MPa at 2100 RPM. This shows that the higher the rotational speed, the greater the internal load borne by the material due to centrifugal force and friction between bearing elements [21].

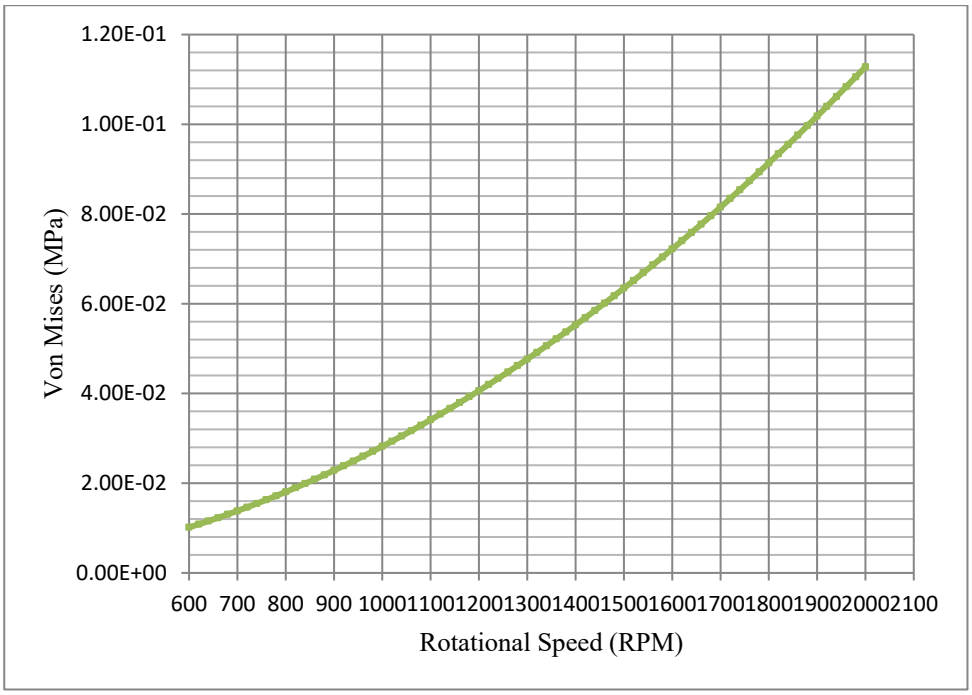

Fig. 3. Von Mises stress on SAE 52100 type bearings without lubrication

As shown in Figure 4, the ANSYS simulation shows that increasing speed leads to wider, more concentrated Von Mises stress, especially at the inner ring and ball contact area, with critical stress levels reaching 2.43×10^6 to 4.47×10^6 Pa [22]. High-speed operation causes metal-to-metal friction, elevated temperatures, and significant local deformation [23]. At 2000 RPM, increased inertial forces sharply raise compressive stress, risking plastic deformation, microcracks, and fatigue failure [24]. Stress rises due to both dry friction and centrifugal force, which grows quadratically with speed. Despite SAE 52100's strength, its elastic limit can be exceeded under prolonged stress. Solutions include applying effective lubrication, optimizing surface geometry or coatings, and monitoring operating conditions to prevent failure [25].

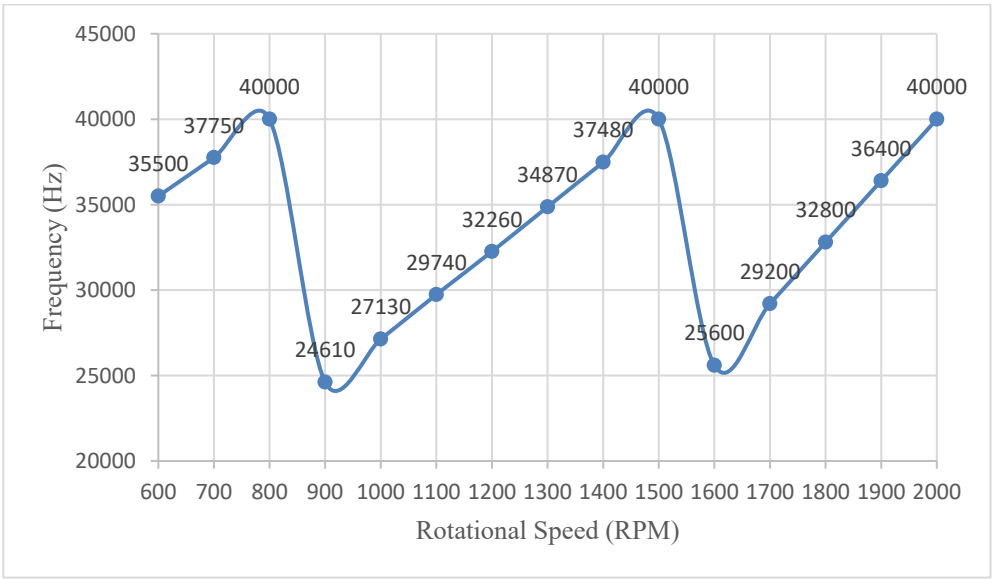

Fig. 4. Frequency on SAE 52100 type bearings without lubrication

This phenomenon indicates resonance, where rotational speed approaches the bearing's natural frequency, causing excessive dynamic deformation. ANSYS results show a sharp increase in stress and deformation at certain speeds, especially in the ball path and inner ring. The absence of lubrication removes damping, making the system more prone to resonance and stress spikes. Increased RPM also alters mass distribution and stiffness, shifting natural frequencies during operation [26]. This raises the risk of fatigue, wear, and structural failure, particularly in critical environments. Solutions include active lubrication systems, vibration dampers, and structural redesign to avoid frequency overlap and minimize resonance effects [27].

Deformation Analysis

As shown in Figure 1, as speed increases from 800 to 2000 RPM, deformation in the ball bearing raceway becomes more widespread and severe, shifting from light blue to reddish-yellow zones. Without lubrication, direct metal contact causes higher friction, local heat, and increased contact pressure, leading to significant elastic deformation and potential bearing failure [28]. This condition shortens bearing life, increases vibration, and threatens operational stability. Solutions include applying an appropriate lubrication system, performing periodic balancing, selecting high-fatigue-strength materials, and enhancing surface quality [29]. Understanding deformation distribution is essential for designing optimal lubrication, materials, and operating conditions for SAE 52100 bearings in high-speed applications [30].

As shown in Figure 2, as speed increases from 600 to 2000 RPM, the equivalent elastic strain in SAE 52100 bearings grows significantly, with strain distribution shifting from dark blue to reddish-yellow, indicating rising contact pressure and deformation. Metal-to-metal friction becomes dominant, causing increased heat, wear, and risk of fatigue failure [19]. This reduces bearing life, increases vibration, and lowers energy efficiency. Solutions include applying proper lubrication, regular maintenance, material and surface optimization, and rotational balancing [20].

As shown in Figure 3, based on the simulation results of Von Mises stress against rotational speed (RPM) on SAE 52100 type bearings without lubrication. There is a significant increase in stress as the RPM increases. The graph shows a non-linear curve that tends to be exponential, where the Von Mises stress increases from around 1.00×10^{-2} MPa at 600 RPM to almost 1.15×10^{-1} MPa at 2100 RPM. This shows that the higher the rotational speed, the greater the internal load borne by the material due to centrifugal force and friction between bearing elements [21].

As shown in Figure 4, the graph shows a fluctuating pattern where the frequency value experiences sharp cycles of ups and downs in the speed range of 600 to 2000 RPM. For example, at 800 RPM, the frequency reaches a peak value of 40,000 Hz, then drops drastically to 24,610 Hz at 900 RPM, and then increases gradually to another peak of 40,000 Hz at 1500 RPM, before dropping again to 25,600 Hz at 1600 RPM, and again increasing to 40,000 Hz at 2000 RPM.

Vibration Analysis

As shown in Figure 5, based on the results of vibration amplitude simulations on SAE 52100 type bearings without lubrication. As shown in Figure 5, a significant increase in amplitude is observed at rotational speeds of around 1100 RPM. The graph shows that the highest amplitude occurs in the inner bearing section at around 1.55×10^{-5} mm, followed by the ball bearing section at around 8.5×10^{-6} mm, and the outer bearing section with a much

smaller amplitude, which is around 2.2×10^{-6} mm. This amplitude spike indicates the presence of local structural resonance, which is a strong indication that at these speeds, the bearing system experiences excessive vibration due to the excitation of the natural frequency of the components [28].

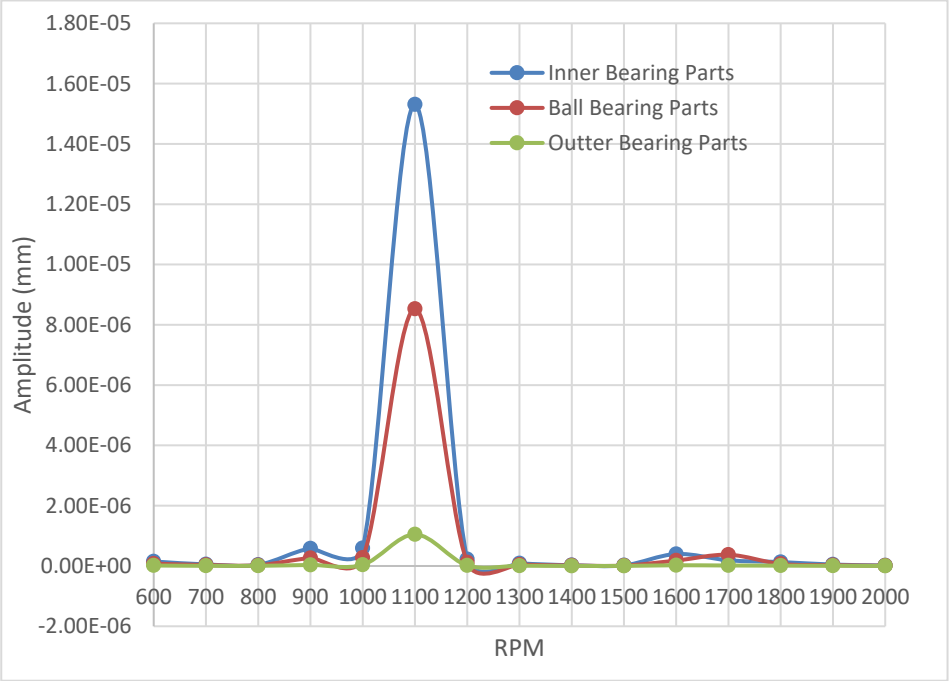

Fig. 5. Vibration amplitude on SAE 52100 type bearings without lubrication

This phenomenon, confirmed by ANSYS simulation, shows that at a critical speed (\~1100 RPM), maximum deformation and elastic strain occur in the inner race and cage of the bearing, with deformation reaching 2.5×10^{-5} mm and strain nearing 6.5×10^{-5} mm. The absence of lubrication causes direct metal contact, increasing friction, temperature, and vibration, especially in areas under high radial forces [26]. This leads to accelerated damage, fatigue failure, and reduced bearing life. Solutions include applying effective lubrication to reduce contact and vibration, implementing vibration monitoring to avoid critical speeds, and optimizing bearing design and material selection [29].

IV. Conclusions

This study demonstrates that the absence of lubrication in SAE 52100 bearings significantly increases deformation, equivalent elastic strain, Von Mises stress, and vibration amplitude as rotational speed increases from 600 to 2000 RPM. The results show that strain and stress concentrations are especially prominent in the inner raceway and ball contact areas, with critical values approaching the material's elastic limit. Resonance conditions were also identified around 1100 RPM, indicating a strong correlation between excitation frequency and structural vibration modes. These findings confirm that high-speed dry operation exacerbates wear, increases the likelihood of fatigue failure, and compromises overall system stability.

To mitigate these issues, the implementation of an effective lubrication system is essential, particularly for high-speed applications. Lubrication not only reduces friction and temperature rise but also acts as a damping medium to prevent resonance amplification. Additional strategies include periodic vibration monitoring to avoid critical speeds,

structural redesign of the bearing to decouple natural frequencies, and the use of advanced materials or surface treatments to enhance fatigue resistance. These combined approaches can improve the operational reliability and service life of high-performance bearing systems.

This study can be extended by incorporating transient loading conditions, variable-speed operation, and thermal effects into the simulation model. Experimental validation of the simulation results is also recommended to strengthen the applicability of the findings to real-world industrial systems.

References

[1] K.J. Dogahe, V. Guski, M. Mlikota, S. Schmauder, W. Holweger, J. Spille *et al.*, "Simulation of the fatigue crack initiation in SAE 52100 martensitic hardened bearing steel during rolling contact," *Lubricants*, vol. 10, no. 4, p. 62, Apr. 2022, doi: 10.3390/lubricants10040062.

[2] R.N. Amrullah, S. Hadi, and M.A. Rizza, "Simulation-based methodology to investigate the impact of material type and compressive speed variation on effective strain rate and springback," *Journal of Mechanical Engineering Science and Technology (JMEST)*, vol. 8, no. 2, pp. 229–239, 2024, doi: 10.17977/um016v8i22024p229.

[3] T. Budiarta, H. Puspito Buwono, and R. N. Amrullah, "Investigation of the influence of warhead shape and type of missile weapon material counter-training tank weapons simulation approach," *Journal of Mechanical Engineering Science and Technology (JMEST)*, vol. 9, no. 1, pp. 39–51, 2025, doi: 10.17977/um016v9i12025p039.

[4] L.D. Saputra and E. Yudiyanto, "Toolpath motion strategy and feed rate in CNC milling on energy consumption of machining process," *Journal of Mechanical Engineering Science and Technology (JMEST)*, vol. 9, no. 1, pp. 114–125, 2025, doi: 10.17977/um016v9i12025p114.

[5] R.R. Dwi Ananto and Andoko, "Coil spring type analysis using the finite element method," *IOP Conf Ser Mater Sci Eng*, vol. 1034, no. 1, p. 012016, Feb. 2021, doi: 10.1088/1757-899x/1034/1/012016.

[6] C. Sferrazza and R. D'Andrea, "Sim-to-real for high-resolution optical tactile sensing: from images to three-dimensional contact force distributions," *Soft Robot*, vol. 9, no. 5, pp. 926–937, Oct. 2022, doi: 10.1089/soro.2020.0213.

[7] Z. Cheng, K. Huang, Y. Xiong, and M. Sang, "Dynamic analysis of a high-contact-ratio spur gear system with localized spalling and experimental validation," *Machines*, vol. 10, no. 2, p. 154, Feb. 2022, doi: 10.3390/machines10020154.

[8] M.M. Atef, W. Khair-Eldeen, J. Yan, and M.G.A. Nassef, "Investigating the combined effect of multiple dent and bump faults on the vibrational behavior of ball bearings," *Machines*, vol. 10, no. 11, p. 1062, Nov. 2022, doi: 10.3390/machines10111062.

[9] D. Ruan, Y. Chen, C. Gühmann, J. Yan, and Z. Li, "Dynamics modeling of bearing with defect in modelica and application in direct transfer learning from simulation to test bench for bearing fault diagnosis," *Electronics (Basel)*, vol. 11, no. 4, p. 622, Feb. 2022, doi: 10.3390/electronics11040622.

[10] J. Mohammed and J. Abdulhady, "Rolling bearing fault detection based on vibration signal analysis and cumulative sum control chart," *FME Transactions*, vol. 49, no. 3, pp. 684–695, 2021, doi: 10.5937/fme2103684M.

[11] X. Yuan, N. Azeem, A. Khalid, and J. Jabbar, "Vibration energy at damage-based statistical approach to detect multiple damages in roller bearings," *Applied Sciences*, vol. 12, no. 17, p. 8541, Aug. 2022, doi: 10.3390/app12178541.

[12] W. Song, L. Guo, A. Duan, H. Gao, Y.Yu, T. Feng *et al.*, "Multispectral balanced automatic fault diagnosis for rolling bearings under variable speed conditions," *Struct Control Health Monit*, vol. 2023, pp. 1–17, Oct. 2023, doi: 10.1155/2023/9369850.
[13] Y.B. Guo and C.R. Liu, "Mechanical properties of hardened AISI 52100 steel in hard machining processes," *J Manuf Sci Eng*, vol. 124, no. 1, pp. 1–9, Feb. 2002, doi: 10.1115/1.1413775.
[14] Z. Shi, J. Li, X. Zhang, C. Shang, and W. Cao, "Influence mechanisms of inclusion types on rotating bending fatigue properties of SAE52100 bearing steel," *Materials*, vol. 15, no. 14, Jul. 2022, doi: 10.3390/ma15145037.
[15] P. Zmarzły, "Multi-dimensional mathematical wear models of vibration generated by rolling ball bearings made of AISI 52100 bearing steel," *Materials*, vol. 13, no. 23, p. 5440, Nov. 2020, doi: 10.3390/ma13235440.
[16] T. Sorgente, S. Biasotti, G. Manzini, and M. Spagnuolo, "A survey of indicators for mesh quality assessment," *Computer Graphics Forum*, vol. 42, no. 2, pp. 461–483, May 2023, doi: 10.1111/cgf.14779.
[17] R. Turnbull, N. Dolatabadi, R. Rahmani, and H. Rahnejat, "Nonlinear tribodynamics of an elastic shaft with a flexible bearing outer race," *Proceedings of the Institution of Mechanical Engineers, Part K: Journal of Multi-body Dynamics*, vol. 237, no. 2, pp. 290–306, Jun. 2023, doi: 10.1177/14644193231161136.
[18] C. Lei, F. Li, B. Gong, and X. Jia, "An integrated model to characterize comprehensive stiffness of angular contact ball bearings," *Math Probl Eng*, vol. 2020, 2020, doi: 10.1155/2020/4951828.
[19] R. Turnbull, R. Rahmani, and H. Rahnejat, "The effect of outer ring elastodynamics on vibration and power loss of radial ball bearings," *Proceedings of the Institution of Mechanical Engineers, Part K: Journal of Multi-body Dynamics*, vol. 234, no. 4, pp. 707–722, Dec. 2020, doi: 10.1177/1464419320951398.
[20] A. Elgazzar, S.-J. Zhou, J.-H. Ouyang, Z.-G. Liu, Y.-J. Wang, and Y.-M. Wang, "A critical review of high-temperature tribology and cutting performance of cermet and ceramic tool materials," *Lubricants*, vol. 11, no. 3, p. 122, Mar. 2023, doi: 10.3390/lubricants11030122.
[21] R. Kumar, I. Hussainova, R. Rahmani, and M. Antonov, "Solid lubrication at high temperatures—A review," Mar. 01, 2022, *MDPI*. doi: 10.3390/ma15051695.
[22] J. Lei, B. Su, S. Zhang, H. Yang, and Y. Cui, "Dynamics-based thermal analysis of high-speed angular contact ball bearings with under-race lubrication," *Machines*, vol. 11, no. 7, p. 691, Jul. 2023, doi: 10.3390/machines11070691.
[23] D. Calegaro, M. Merli, G. Ferrari, and S. Mariani, "Fatigue-induced failure of polysilicon MEMS: nonlinear reduced-order modeling and geometry optimization of on-chip testing device," *Micromachines (Basel)*, vol. 15, no. 12, p. 1480, Dec. 2024, doi: 10.3390/mi15121480.
[24] H. Demirpolat, R. Binali, A. D. Patange, S.S. Pardeshi, and S. Gnanasekaran, "Comparison of tool wear, surface roughness, cutting forces, tool tip temperature, and chip shape during sustainable turning of bearing steel," *Materials*, vol. 16, no. 12, p. 4408, Jun. 2023, doi: 10.3390/ma16124408.
[25] F. Dua, D. Li, X. Sa, C. Li, Y. Yu, C. Li *et al.*, "Overview of friction and wear performance of sliding bearings," *Coatings*, vol. 12, no. 9, p. 1303, Sep. 2022, doi: 10.3390/coatings12091303.
[26] D. Pietrusiak, J. Wróbel, M. Czechowski, and W. Fiebig, "Dynamic NVH numerical analysis of power steering in the presence of lubricant in the system," *Materials*, vol. 15, no. 7, p. 2406, Mar. 2022, doi: 10.3390/ma15072406.

[27] L.H.M. Palmeth, J.G.A. Marin, and D.C.P. Montiel, "Structural and dynamic evaluation of a test bench for mechanical vibrations using finite elements," *International Journal of Innovative Research and Scientific Studies*, vol. 7, no. 3, pp. 1205–1215, May 2024, doi: 10.53894/ijirss.v7i3.3217.
[28] K. Laxmikant, N.H. Padmaraj, N. Khan, P.E. Jagadeesha, R. Pradeep, and K.N. Chethan, "Analysis of vibration signature in deep groove ball bearing using finite element method," *Journal of Applied Engineering Science*, vol. 20, no. 3, pp. 861–869, 2022, doi: 10.5937/jaes0-33912.
[29] B. Wan, J. Yang, and S. Sun, "A method for monitoring lubrication conditions of journal bearings in a diesel engine based on contact potential," *Applied Sciences*, vol. 10, no. 15, p. 5199, Jul. 2020, doi: 10.3390/app10155199.
[30] A. Chavan and V. Sargade, "Surface integrity of AISI 52100 steel during hard turning in different near-dry environments," *Advances in Materials Science and Engineering*, vol. 2020, no. 1, Jan. 2020, doi: 10.1155/2020/4256308.